

Connection between vibrational dynamics and topological order in simple glasses

S. I. Simdyankin and M. Dzugutov

*Department of Numerical Analysis and Computer Science,
Royal Institute of Technology, SE-100 44 Stockholm, Sweden*

S. N. Taraskin and S. R. Elliott

Department of Chemistry, University of Cambridge, Lensfield Road, Cambridge CB2 1EW, UK

(Dated: November 20, 2018)

We compare vibrational dynamics in two structurally distinct, simple monatomic model glasses simulated by molecular dynamics: the Lennard-Jones glass with an fcc-related structure and a glass with predominantly icosahedral short-range order. The former, characterized by a single local quasi-periodicity, supports only modes with acoustic behaviour. In the latter, the presence of optic modes and two incommensurate length scales is observed. This pattern of vibrational dynamics is shown to be closely related to that of a Frank-Kasper crystal having the same local topological order.

PACS numbers: 63.50.+x, 61.43.Bn, 81.05.Kf

I. INTRODUCTION

The nature of vibrational dynamics in topologically disordered solids remains an unsolved problem of fundamental interest. An important question is to what extent is the vibrational behaviour determined by the atomic structure in such materials. Liquids and glasses lack global symmetry, and, therefore, their vibrational eigenstates are no longer phonons. Nevertheless, long-wavelength phonon-like propagating acoustic plane waves can be observed in these structures^{1,2} up to a certain frequency, known as the Ioffe-Regel crossover ω_{IR} , beyond which they are heavily damped due to strong scattering. However, the spectral functions (e.g. the dynamical structure factor $S(Q, \omega)$) are still peak-shaped even beyond ω_{IR} (see e.g. Ref.^{1,2} and references therein). Thus, the concept of dispersion, as peak-position frequency versus the wavevector magnitude, is still valid in disordered structures^{1,2,3,4,5,6,7}. In glasses, it has been assumed that the position of the main maximum, Q_0 , of the static structure factor $S(Q)$ plays the role of the first reciprocal-lattice point, with the first pseudo-Brillouin zone extending up to $Q_0/2$ ^{3,4,8,9}.

However, the main maximum of $S(Q)$, manifesting the dominant pseudo-periodicity in glasses, does not contain full information about the glass structure. Even in simple monatomic liquids and glasses, there exist distinct types of short-range order (SRO) closely related to the respective counterpart periodic structures¹⁰. Then, to what extent is the structural diversity of glasses reflected in their vibrational properties? In particular, can the distinctive features of the vibrational dynamics characteristic of a crystalline structure be discerned in the vibrational properties of a glass with similar local order?

A type of SRO that is most interesting in this respect is that based on icosahedral coordination of the first shell of neighbors. It is commonly associated with the glass-forming ability of simple metallic systems¹¹. The frustration inherent in packing icosahedra in Euclidean (flat) 3D space in the liquid state produces 6-fold defects which,

on cooling, form disclination lines. The latter may align in space, forming globally ordered patterns, e.g. Frank-Kasper periodic phases or morphologically related quasicrystals. Under sufficiently rapid cooling, the disclination lines get entangled, forming a glass¹¹.

The large numbers of atoms in the primitive cells of the Frank-Kasper phases give rise to many optic vibrational modes. Can these modes survive the lack of long-range order in the related glass? In addressing this issue, it is important to discriminate between the optic modes arising as a result of a particular type of topological SRO, of interest here, and those induced by the chemical SRO in a system with more than one type of atom. The latter have been observed in simple glassy alloys^{12,13}.

Here, we employ molecular dynamics to investigate the vibrational dynamics in a monatomic model of a glass with icosahedral SRO (IC glass)¹⁴. The thermodynamically stable solid phase on freezing for this system is a dodecagonal quasicrystal¹⁵, whereas the energy-favored structure is the σ phase^{16,17,18}, a Frank-Kasper crystal¹⁹.

The rest of the paper is arranged as follows. In Sec. II, we describe simulation procedure. The results and their discussion are presented in Sec. III and Sec. IV, respectively. The conclusions are given in Sec. V.

II. SIMULATION

The IC glass was obtained in the course of a NVE molecular dynamics (MD) simulation. A system of 16000 particles was cooled from the liquid state above the melting point $T_m \simeq 0.5$ at a constant density $\rho = 0.8771$ (all quantities reported here are expressed in the Lennard-Jones reduced units²⁰ defining the pair potential¹⁴). This is the minimum energy density at zero pressure in the σ phase¹⁷. We cooled the system in a stepwise manner. At each cooling step, the temperature of the system was reduced by scaling the velocities of the constituent particles. Then the system was equilibrated at constant temperature until the decrease of the poten-

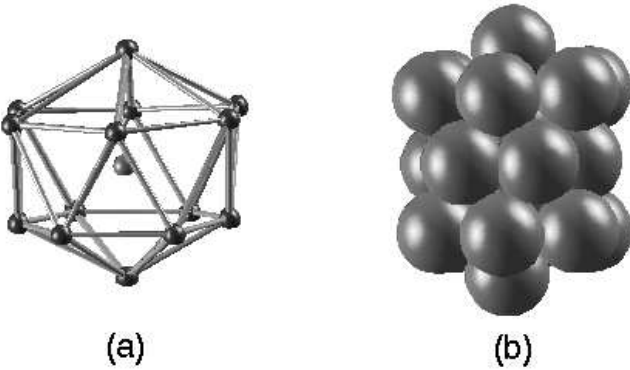


FIG. 1: (a) Frank-Kasper Z14 polyhedron. (b) A fragment of the -72° disclination line (two interpenetrating Z14 elements) as observed in the simulated IC glass.

tial energy was observed to cease, indicating that a state of metastable equilibrium had been reached. Successful equilibration of this system in the metastable liquid domain below the melting point was possible due to the complexity of its crystallization pattern, significantly inhibiting the process of crystalline nucleation. The equilibration time rapidly increased with decreasing temperature. At $T \simeq 0.3$, this time exceeded the time of the simulation run. Below $T = 0.3$, we found that the equilibration had not been completed after the relaxation run of $t = 10^7 \Delta t$, $\Delta t = 0.01$. At this point, the system, therefore, was assumed to be in the glassy state. Then it was cooled to the temperature $T = 0.01$ at which the atoms vibrate around their equilibrium positions and do not diffuse away, and their vibrational dynamics was investigated.

Mindful of the possible growth of crystalline grains in the process of glass formation, we analyzed the evolution of the six-fold structural elements, the Frank-Kasper Z14 polyhedra (shown in Fig. 1(a)). In the process of Frank-Kasper crystallization, interpenetrating Z14 elements form -72° disclination lines (Fig. 1(b)) which eventually thread the entire sample¹¹. Therefore, the extent of crystallization can be assessed by monitoring the length of these disclination lines. Table I demonstrates that the process of glass formation in the IC system is not accompanied by any significant growth of the crystalline phase.

As a reference, we simulated a monatomic Lennard-Jones (LJ) glass with the SRO related to the face-centered cubic (fcc) structure. This glass was prepared at the density $\rho = 1.0888$, corresponding to the zero-pressure energy minimum of the fcc crystal with the LJ potential truncated at $r_c = 4$, by rapidly quenching a system of 16000 particles from a well-equilibrated liquid state at $T = 3$ to $T = 0.01$. The structural distinction between the two glasses is demonstrated in Fig. 2.

In order to gain an insight into the vibrational properties of the IC glass, we also studied the dynamics of a one-component model of the σ phase¹⁷. The latter model

number of Z14 atoms in the disclination line	number of disclination lines		
	$T = 1.0$	$T = 0.5$	$T = 0.3$
1	149	260	599
2	3	27	145
3	0	4	28
4	0	2	9
5	0	0	2
total number of Z14 atoms	155	334	1019

TABLE I: Temperature dependence of the statistics of -72° disclination lines in the IC glass.

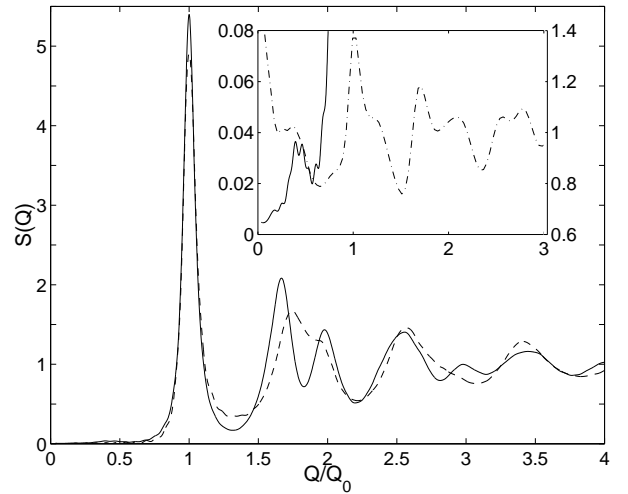


FIG. 2: Static structure factors $S(Q)$ for the IC glass (solid line) and the LJ glass (dashed line). The inset shows the small- Q part of $S(Q)$ (solid line, left-hand scale) and the partial structure factor calculated for the centers of icosahedra (dash-dotted line, right-hand scale), both for the IC glass. ($Q_0 \rho^{-1/3} \simeq 7.17$ and 7.08 for IC and LJ glass, respectively.)

utilized the same pair potential as the IC-glass model. Both models were studied at the same density.

We associated longitudinal vibrational modes with non-zero frequency maxima in the dynamical structure factor, $S(Q, \omega)$, the spectrum of the density-fluctuation time-autocorrelation function²¹: $S(Q, \omega) = N^{-1} \int_0^\infty dt e^{i\omega t} \langle \rho(\mathbf{Q}, t) \rho(-\mathbf{Q}, 0) \rangle$, where $\rho(\mathbf{Q}, t) = \sum_{k=1}^N \exp[-i\mathbf{Q} \cdot \mathbf{r}_k(t)]$ and $\mathbf{r}_k(t)$ is the positional vector of the particle k . For transverse vibrational modes, we calculated the spectra of the transverse current fluctuations²¹: $C_t(Q, \omega) = Q^2 N^{-1} \int_0^\infty dt e^{i\omega t} \langle j_t(\mathbf{Q}, t) j_t(-\mathbf{Q}, 0) \rangle$, where $j_t(\mathbf{Q}, t)$ is the transverse component of the Fourier-transform of the local current: $j_t(\mathbf{Q}, t) = \sum_{k=1}^N (\mathbf{e}_t \cdot \mathbf{v}_k(t)) \exp[-i\mathbf{Q} \cdot \mathbf{r}_k(t)]$, $\mathbf{e}_t \perp \mathbf{Q}$ and $\mathbf{v}_k(t)$ is the velocity of particle k . Finite-time truncation effects in the spectra of the time-correlation functions were reduced by convolution with a Gaussian window function.

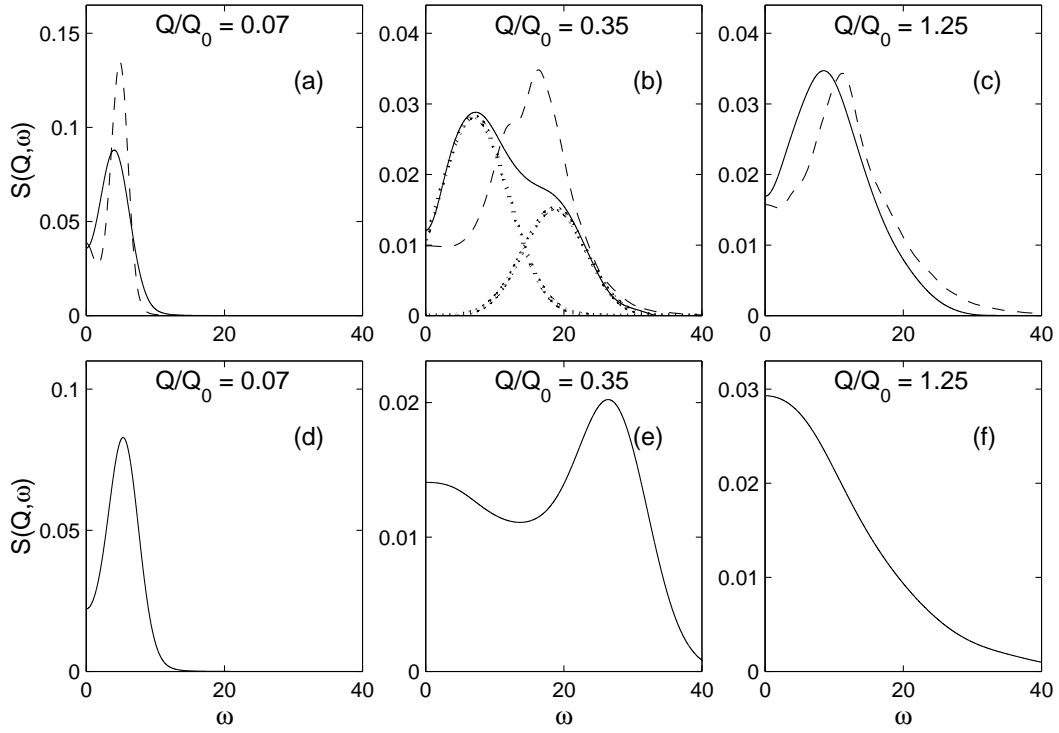


FIG. 3: Dynamical structure factors in the simulated systems at three values of wavenumber as marked. (a)-(c): IC glass, solid line; dashed line, σ phase. In (b), the dotted curves show two Gaussians, the sum of which is fitted to the solid curve; this fit, if plotted, is indistinguishable from the solid curve. (d)-(f): LJ glass.

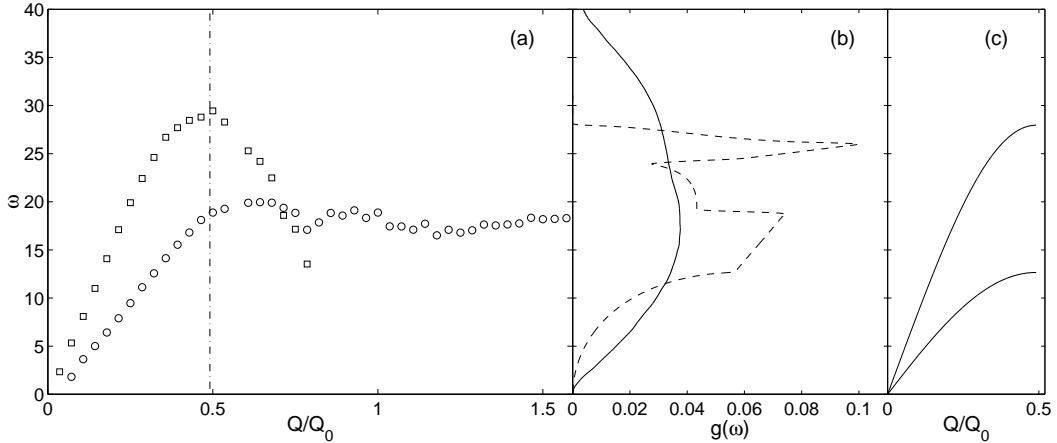


FIG. 4: (a) Dispersion of vibrational excitations for the LJ glass. Open squares: longitudinal branch. Open circles: transverse branch. Dash-dotted line: the first Brillouin-zone boundary for the fcc structure in the (111) symmetry direction. (b) Vibrational density of states for the LJ glass (solid curve) and for the fcc structure (dashed curve). (c) Phonon-dispersion curves for the fcc structure in the (111) symmetry direction.

III. RESULTS

Fig. 3 shows $S(Q, \omega)$ for the two glassy models, as well as the σ phase, for several representative values of Q . For sufficiently small Q , both glassy systems clearly exhibit acoustic modes which manifest themselves as pronounced Brillouin peaks in $S(Q, \omega)$, Fig. 3(a). A marked differ-

ence between the two sets of curves arises for $Q \gtrsim 0.2 Q_0$. The width of the Brillouin peak in the LJ glass becomes comparable with that of the whole vibrational spectrum (see Fig. 3(e)) and for larger Q the peak disappears (Fig. 3(f)). For the IC glass, a well-defined Brillouin peak persists well beyond Q_0 (Fig. 3(c)). Another important feature of the IC glass is that, for $Q > 0.2 Q_0$,

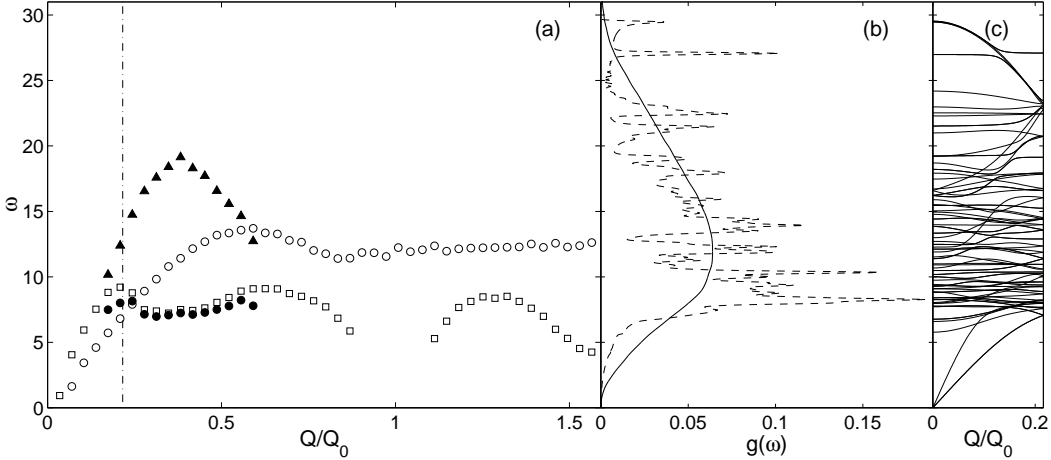


FIG. 5: (a) Dispersion of vibrational excitations in the IC glass. Open squares: longitudinal branch. Open circles: transverse branch. Solid circles and triangles: maxima positions of the two Gaussians approximating $S(Q, \omega)$. Dash-dotted line: the first Brillouin zone boundary for the σ -phase structure in the (001) symmetry direction. (b) Vibrational densities of states of the IC glass (solid line), and the σ -phase structure (dashed line). (c) Phonon-dispersion curves for the σ -phase structure in the (001) symmetry direction.

the Brillouin maximum develops a well-defined shoulder on the high-frequency side (Fig. 3(b)). We analyzed this structure of the Brillouin peak by fitting it with the sum of two Gaussians.

The assumed interpretation of the shoulder observed in the Brillouin peak in $S(Q, \omega)$ of the IC glass as indicating the presence of a separate maximum can be corroborated by a comparison with the structure of $S(Q, \omega)$ calculated for the σ phase which is also shown in Fig. 3(a)-(c). $S(Q, \omega)$ for the σ phase was computed at $T = 0.8$ in the same way as for the glassy systems: the averaging was performed over all wavevectors \mathbf{Q} confined to a narrow spherical shell in reciprocal space, such that $|\mathbf{Q}| \simeq Q$. For $Q/Q_0 = 0.35$, $S(Q, \omega)$ exhibits a pronounced peak at the frequency close to the position of the shoulder observed in $S(Q, \omega)$ of the glassy phase. The two sets of curves in Fig 3(a)-(c) clearly show certain similarities: the number of peaks is the same and their corresponding positions are close. This leads us to the conclusion that the shape of the dynamical structure factor in the frequency domain for the IC glass is generically related to that for its crystalline counterpart, the σ phase. Namely, the peaks in $S(Q, \omega)$ for the IC glass originate from the corresponding peaks for the σ phase, which are broadened and shifted by disorder-induced level-repelling effects²². The level-repelling and hybridization effects describe a reconstruction of the crystalline vibrational spectrum to give the disordered one. These should give rise to a shift of the low-frequency crystalline peaks downwards in frequency but upwards for the high-frequency peaks (see Ref.²² for more detail). Such tendencies are indeed seen in Fig. 3(a)-(c) for the relative positions of the peaks for the σ phase and the IC glass. Therefore, our results support the conjecture that disorder-induced level-repelling effects in vibrational states in crystalline counterparts of

topologically disordered structures, such as the IC glass, are responsible for the main features of their vibrational spectrum.

The dispersion relations as derived from the positions of the respective Brillouin maxima for the LJ and IC models are shown in Figs. 4 and 5, respectively. The patterns corresponding to the longitudinal modes in the two glassy systems are strikingly different. The longitudinal dispersion curve for the LJ glass demonstrates a pattern typical for acoustic modes, with a maximum centered at around $Q_0/2$, Fig. 4(a). The dispersion pattern of the single Brillouin peak observed in $S(Q, \omega)$ for the IC system for $Q < 0.2 Q_0$ can also be identified with acoustic behavior. For larger values of Q , we identify two separate dispersion branches associated with the positions of the maxima of the two Gaussians approximating $S(Q, \omega)$, as shown in Fig. 5(a). The main subpeak of the Brillouin maxima exhibits a very weak Q -dependence, resembling the behavior of the optic modes in crystalline solids (Fig. 5). The shoulder observed in the Brillouin peaks of the IC system gives rise to a higher-frequency dispersion branch which exhibits a maximum. However, in contrast to the acoustic-type dispersion observed in the LJ glass, the maximum is located at around $0.4 Q_0$.

IV. DISCUSSION

The pronounced differences in the behavior of the longitudinal modes in these two model glasses can be rationalized by considering the respective modes in the crystalline counterparts - the σ phase in the case of the IC glass, and the fcc crystal in the case of the LJ glass.

The LJ glass is characterized by a single dominant structural repeat distance, manifested by the first peak

of $S(Q)$. It corresponds to the interplanar spacing along the (111) symmetry direction in the fcc structure (i.e., the apex-basal-plane distance in a close-packed tetrahedron). Q_0 being the first reciprocal-lattice point, the first Brillouin-zone boundary is at $Q_0/2$, which corresponds to the maximum in the dispersion curve of the longitudinal acoustic (LA) modes (Fig. 4(a)). As a result of this structural simplicity, the vibrational dispersion pattern in the LJ glass is also simple, with only LA and transverse branches, as in the counterpart crystalline (fcc) structure (Fig. 4(c)) that has just one atom as the basis in the primitive unit cell.

The pattern of longitudinal vibrational modes in the IC glass is considerably more complex (Fig. 5(a)), displaying a low-frequency weakly dispersive branch with the first maximum at $Q/Q_0 \simeq 0.2$. Its dispersion behavior clearly resembles that of the optic modes which dominate this range of frequencies in the vibrational spectra of the σ phase (Fig. 5(c)). In the same domain of Q , the IC glass also exhibits a higher-frequency branch associated with the high-frequency shoulder of the Brillouin peak. As has been mentioned earlier, this shoulder mirrors a peak in $S(Q, \omega)$ of the high-temperature σ phase (Fig. 3(b)). The latter manifests optic modes and therefore we conclude that optic-type modes dominate the vibrational dynamics in the IC glass for $Q/Q_0 > 0.2$. The position of the maximum in the high-frequency branch, $Q/Q_0 \simeq 0.4$, is twice that in the low-frequency branch, $Q/Q_0 \simeq 0.2$. However, both branches are suppressed at $Q = Q_0$ by the influence of the main peak of $S(Q)$.

The appearance of modes in the IC glass, mirroring the optic modes in the corresponding σ -phase crystal (Fig. 5(c)), is a consequence of the type of topological SRO that exists in both structures. The first Brillouin-zone boundary in the σ phase in the (001) symmetry direction is at $Q \simeq 0.2 Q_0$ (Fig. 5(c)), corresponding very closely to the first pseudo-Brillouin-zone boundary value found in the IC glass (Fig. 5(a)). The behavior observed in the IC glass, that the low-frequency branch first peaks at $Q \simeq 0.2 Q_0$ whereas the high-frequency branch peaks at $Q \simeq 0.4 Q_0$, is typical for nonsymmorphic crystalline structures, of which the σ phase is an example (space group $P4_2/mnm$), for \mathbf{Q} in the direction of a screw axis²³. Some modes sense any particular (pseudo-) periodic atomic-density fluctuations, whereas some modes sense alternate such atomic-layer spacings and therefore the apparent first Brillouin-zone boundaries differ by a factor of two. On the other hand, the dominant length scale in the IC glass that is manifested by the main peak of $S(Q)$ corresponds to the layer periodicity in the (111) direction of the σ phase (the same apex-basal-plane distance in tetrahedra as in fcc).

Optic modes in the IC glass give no contribution to $S(Q, \omega)$ for $Q/Q_0 < 0.2$. This is not surprising because the dynamical structure factor describes the response of the system to plane wave excitations. Even in crystals, the optic phonons are not simple plane waves (the atoms inside the unit cell are not displaced accord-

ing to a plane wave), and in the long-wavelength limit ($Q \rightarrow 0$) only acoustic modes respond to plane-wave excitations^{1,2}. The signature of optic-like excitations appears in the dynamic structure factor of the IC glass only when the wavelength becomes comparable with the size of structural units responsible for this effect.

The dispersion curves for the IC glass thus indicate the existence of an additional pseudo-periodic interlayer spacing incommensurate with that manifested by the main peak of $S(Q)$. The latter corresponds to the same pseudo-period in the atomic-density fluctuations as for the LJ glass. The second length scale is related to the interlayer spacing in aggregates of interpenetrating icosahedral units, as along the (001)-axis in the σ phase. This assertion is confirmed by the fact that both the total $S(Q)$ and the partial structure factor calculated only for the centers of icosahedra exhibit a prepeak at $Q \simeq 0.4 Q_0$ (see the inset in Fig. 2). The presence of an additional length scale in the IC glass appears to agree with recent observations of medium-range order in paracrystalline amorphous models^{24,25}. This length scale is associated with a particular type of structural unit which is morphologically close to those found in the counterpart crystalline structure. In a reciprocal-space picture, the effect of these structural units can be analogous to that of the “quasi-Bragg planes”^{26,27} used for explanation of the first sharp diffraction peak in $S(Q)$ of amorphous solids.

The difference in the behaviour of collective vibrational modes in the two glasses is also reflected in their densities of states, Figs. 4(b), 5(b). On the other hand, the curves for the vibrational density of states in both glasses appear to be consistent with the respective curves calculated for the crystalline counterparts.

The dispersion patterns of the transverse modes are qualitatively similar (Figs. 4(a), 5(a)). This implies that either these modes are insensitive to the structure or, more likely, any structure effects cannot be shown using $C_t(Q, \omega)$. This will be analyzed elsewhere.

V. CONCLUSION

In conclusion, we have demonstrated that structural distinctions in simple monatomic glasses give rise to an appreciable difference in the behaviour of vibrational excitations. We have shown that the main features in the dynamical structure factor of the IC glass are generically related to those of its crystalline counterpart, the σ phase. The other distinctive features of vibrational dynamics displayed by the IC glass, namely, the presence of optic-like modes and an additional pseudo-Brillouin zone boundary incommensurate with Q_0 , can be accounted for by the specific structure of aggregates of interpenetrating icosahedra characteristic of the σ phase, which was previously shown¹⁷ to be a good crystalline counterpart of the IC glass. This observation implies that the structural similarity between a glass and its crystalline counterpart extends well beyond the shell of nearest neighbors. The

existence of an additional incommensurate length scale and optic modes may be a generic feature of glasses having complex counterpart crystalline structures.

Swedish research funds: Natural Science Research Foundation (NFR), Technical Research Foundation (TFR), and Network for Applied Mathematics (NTM). S.N.T. is grateful to EPSRC for support.

Acknowledgments

S.I.S. and M.D. thank Trinity College, Cambridge for hospitality, and acknowledge support from the following

¹ S. N. Taraskin and S. R. Elliott, Phys. Rev. B **61**, 12017 (2000).
² S. N. Taraskin and S. R. Elliott, Phys. Rev. B **61**, 12031 (2000).
³ G. S. Grest, S. R. Nagel, and A. Rahman, Phys. Rev. Lett. **49**, 1271 (1982).
⁴ G. S. Grest, S. R. Nagel, and A. Rahman, Phys. Rev. B **29**, 5968 (1984).
⁵ S. N. Taraskin and S. R. Elliott, Europhys. Lett. **39**, 37 (1997).
⁶ M. Sampoli, P. Benassi, R. Dell'Anna, V. Mazzacurati, and G. Ruocco, Phil. Mag. B **77**, 473 (1998).
⁷ R. Dell'Anna, G. Ruocco, M. Sampoli, and G. Viliani, Phys. Rev. Lett. **80**, 1238 (1998).
⁸ J. Hafner, *From Hamiltonians to Phase Diagrams* (Springer-Verlag, Berlin, 1987).
⁹ J.-B. Suck, P. A. Egelstaff, R. A. Robinson, D. S. Silvia, and A. D. Taylor, J. Non-Cryst. Solids **150**, 245 (1992).
¹⁰ F. H. Stillinger and R. A. LaViolette, J. Chem. Phys. **83**, 6413 (1985).
¹¹ D. R. Nelson and F. Spaepen, Solid State Phys. **42**, 1 (1989).
¹² J. Hafner, J. Phys. C **16**, 5773 (1983).
¹³ C. J. Benmore, S. Sweeney, R. A. Robinson, P. A. Egelstaff, and J.-B. Suck, J. Phys.: Condens. Matter **11**, 7079 (1999).
¹⁴ M. Dzugutov, Phys. Rev. A **46**, R2984 (1992).
¹⁵ M. Dzugutov, Phys. Rev. Lett. **70**, 2924 (1993).
¹⁶ M. Dzugutov, Phys. Rev. Lett. **79**, 4043 (1997).
¹⁷ S. I. Simdyankin, S. N. Taraskin, M. Dzugutov, and S. R. Elliott, Phys. Rev. B **62**, 3223 (2000).
¹⁸ J. Roth and A. R. Denton, Phys. Rev. E **61**, 6845 (2000).
¹⁹ F. C. Frank and J. S. Kasper, Acta Cryst. **12**, 483 (1959).
²⁰ M. P. Allen and D. J. Tildesley, *Computer Simulation of Liquids* (Clarendon Press, Oxford, 1987).
²¹ J.-P. Hansen and I. R. McDonald, *Theory of Simple Liquids* (Academic Press, London, 1986), 2nd ed.
²² S. N. Taraskin, Y. L. Loh, G. Natarajan, and S. R. Elliott, Phys. Rev. Lett. Submitted.
²³ W. Steurer, in *Structure of Solids*, edited by V. Gerod (VCH, Weinheim, 1993).
²⁴ M. M. J. Treacy, J. M. Gibson, and P. J. Kebinski, J. Non-Cryst. Solids **231**, 99 (1998).
²⁵ M. M. J. Treacy, P. M. Voyles, and J. M. Gibson, J. Non-Cryst. Solids **266-269**, 150 (2000).
²⁶ A. Uhlherr and S. R. Elliott, J. Phys.: Cond. Mat. **6**, L99 (1994).
²⁷ P. H. Gaskell and D. J. Wallis, Phys. Rev. Lett. **76**, 66 (1996).